Interaction Shock Shape for Transverse Injection in Supersonic Flow

JOSEPH A. SCHETZ*
Virginia Polytechnic Institute, Blacksburg, Va.

This paper is concerned with the development of a capability for predicting the interaction shock shape attending transverse injection in supersonic flow. Both gaseous and liquid injectants are treated. New experimental results for liquid injection at Mach 2.1 are also presented with particular attention directed at the importance of the relation of the injectant vapor pressure to the external pressure in the vicinity of the injection port. For gaseous injection, a new analysis based on an equivalent solid-body concept is presented and substantiated by comparison with experiment over a wide range of conditions. A complementary analysis for liquid injection is also developed and shown to provide reasonable predictions for problems where significant flash vaporization occurs.

Nomenclature

C_D = drag coefficient
d_j = injection port diameter
h = penetration height $\simeq$ vertical distance to the center of the Mach disk for the case of an underexpanded jet
$\dot{m}_j$ = mass flow rate of injectant = $\pi r_j^2 \rho_j u_j$
M = Mach number
P_{eb} = effective back pressure = $0.8\,P_2$
P_j = injection pressure
P_T = total pressure
q = dynamic pressure = $\rho u^2/2$
r_j = injection port radius
R_{b_1} = blast-wave-body nose radius, Eq. (1a)
R_{b_2} = disk-height-body nose radius, Eq. (5)
R_c = shock radius of curvature
u = axial velocity
x = axial distance from upstream edge of injector port or equivalent solid body (except in Fig. 6)
x' = axial distance from center of curvature of the hemispherical nose
y = normal distance from body surface
ρ = density
Δ = shock stand-off distance
β = centerline displacement
Δh_v = heat of vaporization
θ = Mach angle

Subscripts

a = freestream conditions
j = injectant condition

Introduction

THE nature of the interaction between a uniform supersonic stream and a jet of fluid injected transverse to that stream is of interest in several technological applications. Of particular importance are the fields of external missile controls, thrust vector control, and fuel injection in supersonic combustion ramjets. The shape of the shock wave induced in the main stream directly determines the extent and character of the interaction region for the controls applications; for the fuel injection application, it determines the total pressure loss attendant to the injection process.

In the simplest sense, the injected fluid presents an obstruction to the main supersonic stream, which is compressed through a shock wave as it turns to negotiate the obstruction. Formally, it should be possible to calculate the mutual interaction between the injected fluid and the freestream, and to predict not only the interaction shock shape but also the trajectory of the injectant. However, even if such a calculation is limited to inviscid considerations, a problem of unmanageable proportions, including three-dimensional, rotational flows with subsonic, transonic, and supersonic regions, remains. Thus, it seems appropriate to simplify the flow model. Several workers[1-3] have sought to apply the Blast Wave Analogy (BWA), which was developed to provide approximate predictions of shock shapes past blunt bodies, to this problem. Here, the drag of the body in the original analogy is replaced by the increase in streamwise momentum of the injectant. However, the BWA does not provide a means for predicting the shock stand-off distance. Hsia[3] suggested the use of an equivalent solid body to represent the obstruction set up by the injected fluid. Generally, the shape of the equivalent body has been taken as half a hemicylinder. At this stage, one could produce a numerical solution of the interaction shock shape using one of the now common blunt body computer routines, but this sophistication is not justified due to the crudity of the body shape description. Rather, some approximate method of determining the shock shape around the given body shape affords a reasonable approach in conjunction with the simple equivalent body. In the absence of heat exchange, Hsia's expression[3] for the equivalent body nose radius can be written

$$R_b = (4/\pi C_D)^{1/2}(\dot{m}_j/\rho_a u_a)^{1/2} \quad (1)$$

This R_b is essentially identical to the length scale that appears in the direct application of the BWA, namely,

$$R_{b_1} = (\dot{m}_j/\rho_a u_a)^{1/2} \quad (1a)$$

because $(4/\pi C_D)^{1/2}$ is near unity for a typical blunt body. Hsia[3] used the BWA formula to predict the shock shape past a body of the nose radius of Eq. (1). However, the BWA formula does not always give good predictions of the shock shape.

Received May 21, 1969; revision received September 23, 1969. This work was supported by the Propulsion Division, Air Force Office of Scientific Research under Grant AF-AFOSR-1228-67, Model AFOSR-67-1228A, Project Task 9711-01 with Technical Supervision by B. T. Wolfson; and by NASA, Contract R-76 (N. Rekos, RAP) and prepared under Naval Ordnance Systems Command Contract NOw 62-0604-c by Johns Hopkins University, Silver Spring, Md.

* Professor and Chairman; also Consultant at the Applied Physics Laboratory, Johns Hopkins University, Silver Spring, Md. Associate Fellow AIAA.

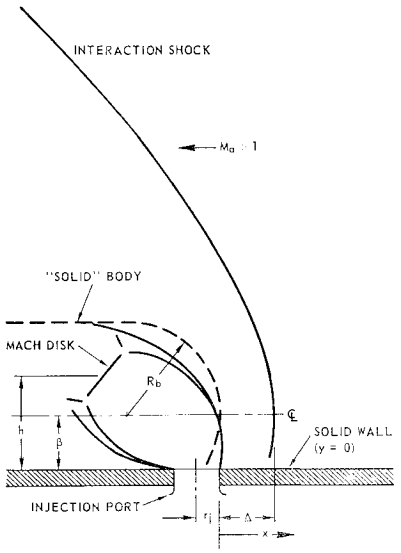

Fig. 1 Schematic of the analytical model.

The implementation of a general equivalent solid-body flow model actually requires two separate elements, and they are best considered individually. First, the size and shape of the equivalent solid body must be related to the injectant and freestream properties of the problem. Second, a simple, reasonably accurate method for calculating the shock shape past the equivalent body must be selected.

We shall treat the second element first, since this aspect of the problem is unaffected by whether the injectant is a gas or a liquid, whereas the definition of the equivalent body is sensitive to that distinction. There are available several approximate procedures for calculating the shock past blunt bodies based upon the equations of motion; however, Billig[4] has presented simple, empirical relations that have proven to be quite accurate.[5] For the problem of interest here, these may be written

$$\frac{x'}{r_j} = \frac{R_b}{r_j} + \left(\frac{\Delta}{R_b}\right)\left(\frac{R_b}{r_j}\right) - \left(\frac{R_c}{R_b}\right)\left(\frac{R_b}{r_j}\right)\times$$

$$\operatorname{ctn}^2(\theta)\left\{\left[1.0 + \left(\frac{y}{r_j}\right)^2\left(\frac{r_j}{R_b}\right)^2\left(\frac{R_b}{R_c}\right)\tan^2\theta\right]^{1/2} - 1.0\right\} \quad (2)$$

where Δ/R_b is the nondimensional stand-off distance given by

$$\Delta/R_b = 0.143\exp(3.24/M_a) \quad (3)$$

and R_c/R_b is the nondimensional radius of the shock at the nose

$$R_c/R_b = 1.143\exp[0.54/(M_a - 1)^{1.2}] \quad (4)$$

(See Fig. 1 for definition of symbols.) The use of these relations should provide a significant improvement over the BWA shock-shape formula, regardless of the method of defining R_b, and they have been adopted here.

In the next section, the relation of the equivalent solid body to the flow properties for gaseous injection is considered. A definition of the solid-body nose radius that is an outgrowth of previous detailed observations of transverse injections[6-8] is presented, and the predicted shock shapes are compared with those found in several experiments. Next, new experimental data for water and Freon 12 injection into a Mach 2.1 stream are presented, and the problem of predicting the interaction shock shape for liquid injection is discussed. Particular attention is drawn to the importance of the injectant vapor pressure in relation to the external pressure in the vicinity of the injection station.

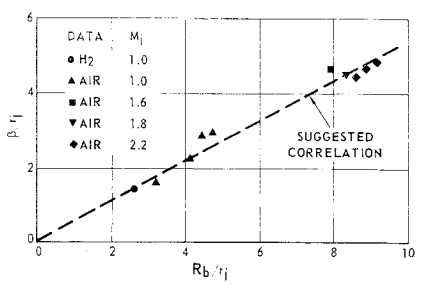

Fig. 2 Shock-wave displacement correlation.

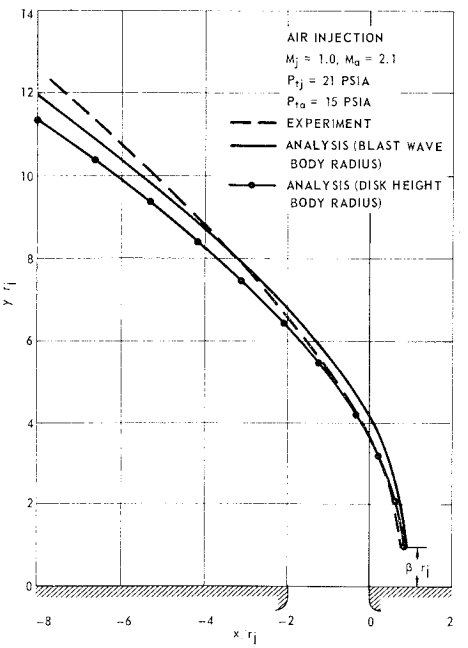

Fig. 3 Shock shape for sonic air injection.

Analysis for Gaseous Injection

Schlieren photographs[6,7] of transverse gaseous injection yield the impression that the equivalent solid body probably should have a roughly spherical nose. A reasonable definition of its radius could be given by Eq. (1) or (1a). An alternative means of relating R_b to the injectant and freestream properties can be developed from studies of the penetration height of the injectant. In most instances, the injectant is underexpanded with respect to its surroundings as it leaves the injection port, and under these conditions,[6-8] experiments showed that the penetration height, h, is essentially equal to the vertical displacement† of the first Mach disk. A length proportional to this height can be chosen as the nose radius. Actually, it was found that a proportionality constant of unity, i.e., $R_{b_2} \equiv h$, was suitable. We may write, for $\gamma_j = \gamma_a = 1.4$ (cases with other values of γ have corresponding expressions),[6,7]

$$h/d_j = R_{b_2}/2r_j = F(M_j)(P_j/P_{eb})^{1/2} \quad (5)$$

where P_j is the jet static pressure and P_{eb} is an "effective back pressure" taken as eight tenths the static pressure behind a normal shock in the freestream. The expression $F(M_j)$ is a function of jet exit Mach number, $F(M_j) = 0.77 M_j + 0.23$. These expressions are simple curve fits to the analysis of Refs. 6 and 7. Either Eq. (5) or Eq. (1a) can be used in conjunction with Eqs. (2–4) to predict the shock shape, and we shall judge the adequacy of both by comparison with experiment. First, though, another feature of the flowfield should be noted. Schlieren photographs[6,7] show

† Since the Mach disk is tilted to the flow, because of downstream bending of the "shock bottle," h is measured to the center of the Mach disk.[6-8]

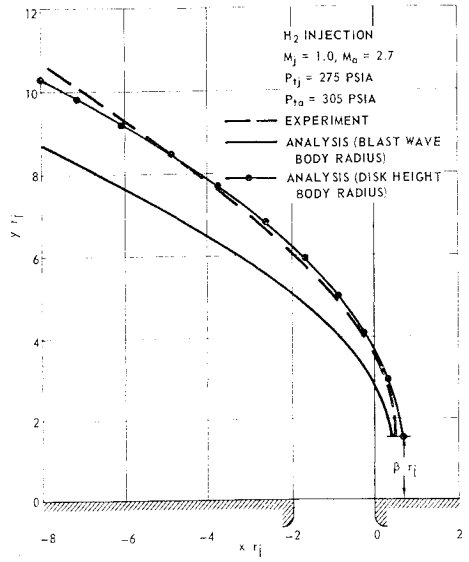

Fig. 4 Shock shape for sonic hydrogen injection.

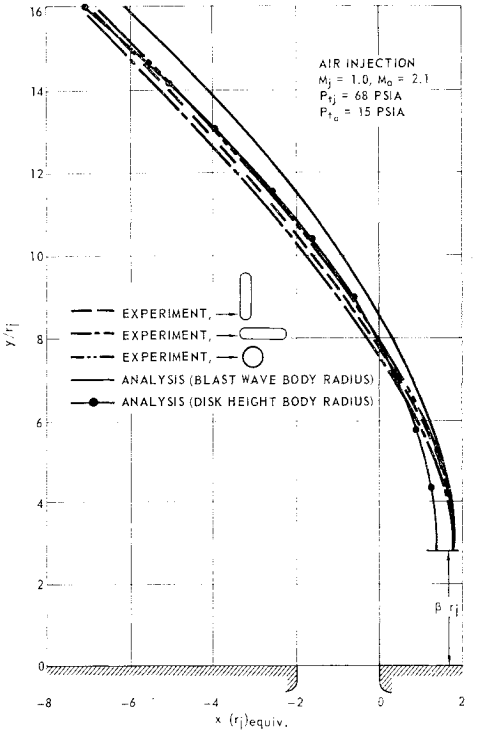

Fig. 5 Shock shapes for various shapes of injection port.

that the interaction shock has an inflection point that is displaced above the solid surface. This can be interpreted to mean that the nose of the "equivalent solid body" is located at a distance β above the surface, and it has been possible to correlate β/r_j vs R_b/r_j; see Fig. 2. (Here R_{b_2}/r_j was used, although an equivalent correlation using R_{b_1}/r_j could easily be generated.)

Figure 3 shows that both analyses provide adequate predictions of stand-off distance and shock shape for the case[6] of sonic air injection through a round port into a Mach 2.1 airstream.

Figure 4 presents comparisons for sonic hydrogen injection into a Mach 2.7 air stream.[8] This case is representative of those important situations where the molecular weights of the injectant and the freestream are widely separated. Here the prediction based on the BWA body radius expression Eq. (1a), is relatively poor, because Eq. (1a) does not account for molecular weight variation. The prediction based on the Mach disk height is good. Moreover, Ref. 9 shows that the shock shape varies with injectant temperature when $\dot{m}_j$ is held constant; Eq. (1a) would not account for this effect, either. An extension of the BWA to account for molecular weight and temperature effects has been proposed.[1] This extension is based upon heuristic reasoning involving a volume-addition effect to the BWA, even though no similar notion is employed in the corresponding application of the BWA to solid bodies. In any event, the use of the correction term of Ref. 1, i.e.,

$$[1 + \{1/(\gamma - 1)M_a^2\}(\rho_a/\rho_j)]^{1/2} \qquad (6)$$

in Eq. (1a) does not fully account for the molecular weight effect observed in the case cited here. This factor has a value of 1.37, while the ratio of R_{b_2} (from the Mach-disk correlation, which provided a good prediction of the shock shape) to the "uncorrected" BWA body radius R_{b_1} [Eq. (1a)] was 1.67.

The third comparison considered here treats the effect of the shape of the injection port on the interaction shock shape. The writer and R. C. Orth have conducted experiments with three injection configurations all having the same cross-sectional area and hence the same flow rate: 1) a round port, 2) a 4 × 1 slot aligned with the main flow, and 3) the same slot aligned perpendicular to the main flow. The interesting experimental result is that the shock shapes produced are similar (Fig. 5). The BWA body radius is based on $\dot{m}_j$ alone and would correctly predict no difference. The disk height correlation used for R_{b_2} was developed for a round port only. However, the experiments just described showed that the location of the first Mach disk in the jet was also insensitive to injector port shape (see Fig. 6), thus this definition of the equivalent body radius also yields the correct qualitative behavior. Figure 5 shows that the quantitative agreement is also quite satisfactory. It is important to note, however, that the experiments permitted only the planform (contour in the x,z plane) of the interaction shock to be determined. Some difference in shock shape in planes other than the plane including the jet trajectory might exist but would go undetected here. Nevertheless, it is surprising that the planform of the shock shape is insensitive to injector port shape over the range considered.

To substantiate the notion that an equivalent solid body has utility for the analysis of secondary injection, a special experiment was conducted. Using the Mach disk definition for the body nose radius, Eq. (5), and the measured vertical displacement of the apparent body center line, β, for the case in Fig. 3, a true solid body was constructed, placed on

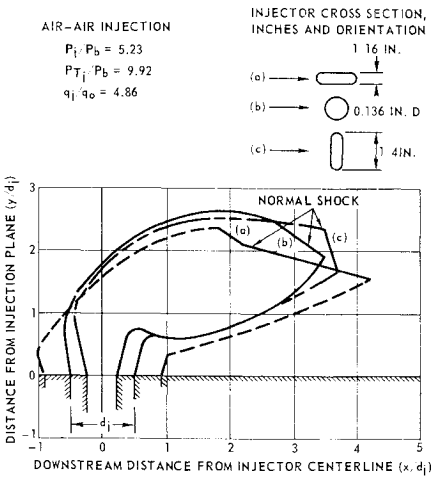

Fig. 6 Effect of injector shape on jet structure for underexpanded sonic injection into a Mach 2.1 supersonic stream.

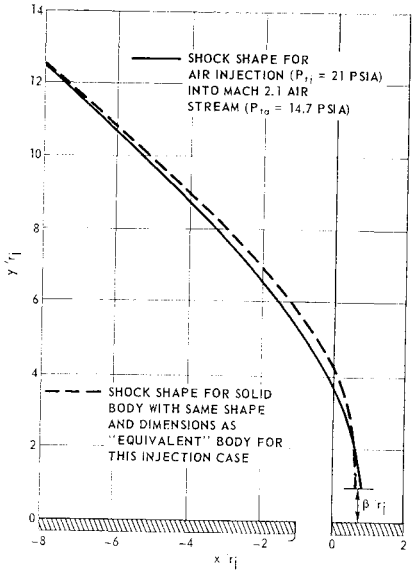

Fig. 7 Shock shapes for an injection experiment with a true solid body corresponding to the "equivalent solid body."

the flat plate used in Ref. 6, and run in the wind tunnel under the same conditions. The resulting "interaction" shock shape was determined and is compared with that measured for the corresponding transverse injection experiment in Fig. 7. The close agreement is apparent.

Liquid Injection Experiments

As a part of an extensive experimental study of transverse liquid injection in supersonic flow where jet break-up and atomization are being observed, interaction shock shapes were determined by 1-msec duration schlieren photographs for several cases of water and Freon-12 injection. The injection model is a simple flat plate that is sting-mounted in an indraft (1-atm stagnation-pressure, 535°R stagnation-temperature), Mach 2.1 wind tunnel. The injectant is brought to a plenum chamber mounted beneath the plate at room temperature and is injected through a small, round port 2 in. from the leading edge and on the center line of the 5-in. span model. The mass flow rate of the injectant was monitored by a rotameter type flow meter. The feed system for the water injection experiments was a simple hook-up to the laboratory water supply passing through a throttling needle valve, while the Freon-12 experiments required a storage tank and air pressurization system.

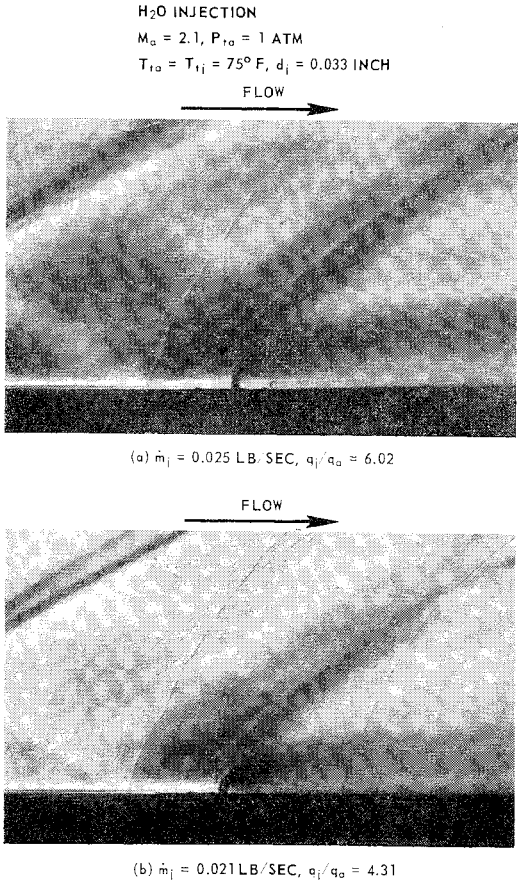

Fig. 8 Schlieren photographs of water injection into a Mach 2.1 airstream.

Typical results for water injection are shown in Fig. 8, where the flow is from left to right. The leading-edge shock, the interaction shock and the initial part of the injected fluid trajectory can be seen. (The spurious lines that run roughly parallel to the interaction shock are caused by the residue of water accumulations on the wind tunnel windows encountered during the tunnel starting process.) For these cases, d_j was 0.033 in. The injectant penetration and the size of the interaction shock are quite sensitive to the injectant-to-free-stream momentum flux ratio. Also, it may be observed that the jet is essentially disintegrated in a distance on the order of 25 diameters.

The flowfield observed for Freon-12 injection through a 0.0185-in.-diam port is shown in Fig. 9. The behavior of the emergent jet and the shape of the interaction shock are quite different from those for the water injection case. Since the pressure felt by the jet as it emerges from the port is much below the injectant vapor pressure, some flash vaporization occurs immediately. This gives the jet the appearance of an underexpanded rocket exhaust plume when it is observed before the tunnel flow is begun. The first part of this plume is visible in the schlieren picture even with the tunnel cross-flow. The jet is then rapidly bent over and proceeds downstream. The interaction shock behaves in a curious fashion in that it has a noticeable bump just above the injection port. Further, the forward, normal portion of the shock appears to intersect the injectant plume rather than lying in front of the injectant altogether. These features of the flow were observed consistently over many tests.

Analysis for Liquid Injection

For the analysis of liquid injection cases, it is necessary to return to the question of the specification of the size and shape of the equivalent "solid" body in terms of the parameters of

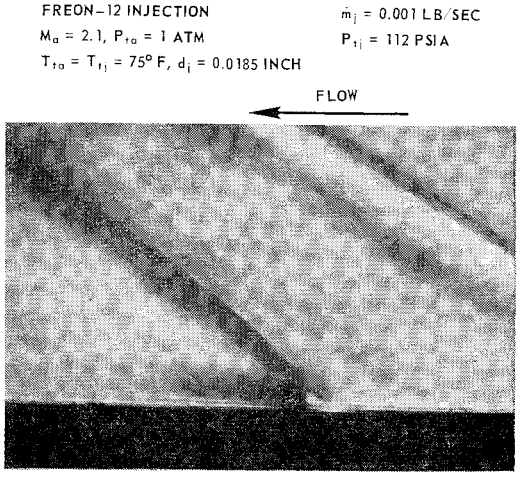

Fig. 9 Schlieren photograph of Freon-12 injection into a Mach 2.1 airstream.

the problem. As discussed previously, a half-hemisphere cylinder with a nose radius essentially equal to the jet penetration height provides good predictions of the shock shape for gaseous injection problems. For liquid injection, a reliable analytical prediction of penetration is not available, so that it is not possible to proceed directly along the same lines as before. However, purely empirical expressions for the penetration height can be employed. The BWA body radius expression (with its inherent limitations) is still available, also, and its application can be tested by comparison with experiment.

For a liquid, the size and shape of the obstruction presented to the main supersonic flow is a direct function of the breakup, atomization and, usually, vaporization of the jet. A fluid that rapidly reaches an all-gaseous state (flash vaporizes) after injection will produce a much blunter obstruction than one that proceeds slowly to a finely atomized or completely vaporized state. Unfortunately, an analytical model for those processes is currently lacking, and it is not practical to develop an equivalent body size and shape expression to account for these effects. Since the BWA expression, Eq. (1a), is not dependent upon whether the injectant is a liquid or gas, the best predictions presumably will be obtained for cases where the injectant vaporizes rapidly and where the temperature and molecular weight of the injectant in the gas phase are similar to those of the freestream.

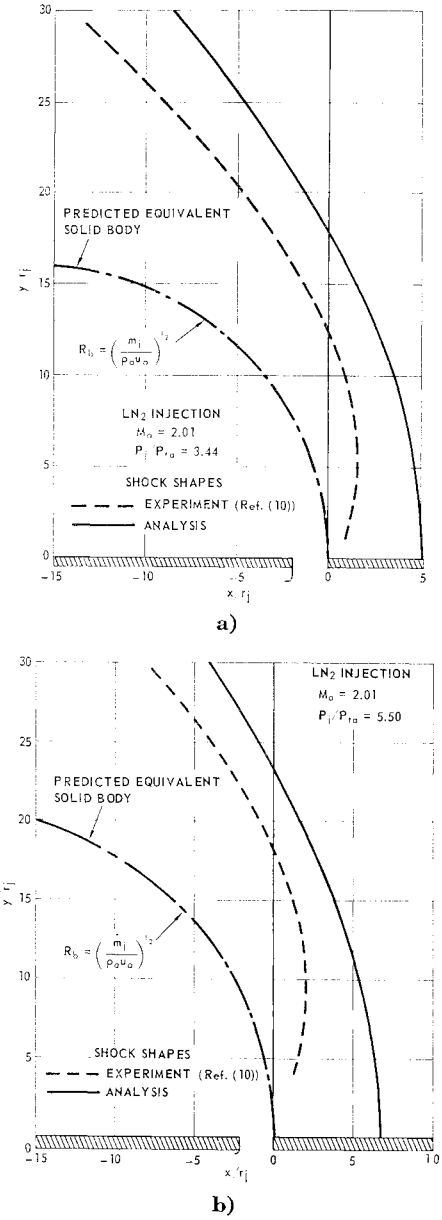

Fig. 10 Shock shapes for liquid nitrogen injection into a Mach 2.01 airstream a) $P_j/P_{ta} = 3.44$ b) $P_j/P_{ta} = 5.50$.

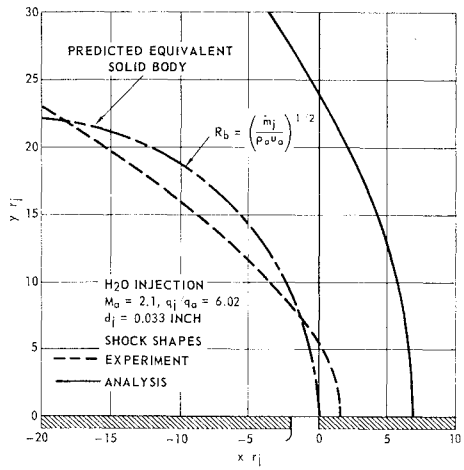

Fig. 11 Overestimation of equivalent solid body and corresponding shock shape for water injection case (no flash vaporization occurs).

Dowdy and Newton[10] presented data on liquid nitrogen injection. Estimates of the portion of the injectant which flash-vaporized are on the order of 10–15%, based upon the extremely conservative assumption that no heat is exchanged between the jet and the surrounding air stream. One might hope, therefore, that the BWA body radius expression would provide reasonable predictions of the shock shape for these cases when used in conjunction with the shock shape formulas of Eqs. (2–4). Comparisons between theory and experiment are given in Figs. 10a and 10b. Also given are the sizes of the predicted equivalent "solid" body for each case. Reasonable agreement is obtained, although the fact that a significant portion of the injectant remains in the liquid state and hence actually causes a smaller obstruction than predicted by the analysis is apparent.

The water injection case reported before was at conditions such that no flash boiling would be present. Thus, the atomization process is dependent upon aerodynamic processes alone and can be expected to proceed relatively slowly. In this instance, a prediction of shock shape that essentially presumes instant vaporization will greatly overestimate the size of the effective obstruction. This is confirmed by the comparison of theory and experiment in Fig. 11. This case provides a convenient standard to assess the utility of an empirical penetration expression for the equivalent body radius. In Ref. 11, an empirical equation is developed that is capable of predicting liquid jet penetration in the absence of flash vaporization, with reasonable accuracy

$$h/d_j = 1.15(\rho_j u_j^2/\rho_a u_a^2)^{1/2} \ln[1 + 6x/d_j] \tag{7}$$

Experimentally, one can observe that the largest part of the penetration is achieved by $(x/d_j) \approx 5$. Using this value, there results for the total penetration

$$h/d_j \simeq 3.95(\rho_j u_j^2/\rho_a u_a^2)^{1/2} \tag{8}$$

It is informative to rewrite this equation so that it can be easily compared in form with Eq. (1a). Thus

$$h \simeq 4.5(u_j/u_a)^{1/2}(\dot{m}_j/\rho_a u_a)^{1/2} \tag{8a}$$

Here we can note a new dependence on the velocity ratio. For a fixed injectant mass flow rate, this is a density-sensitive term, and a strong dependence on injectant density should certainly be present. One can hope then that Eq. (8a) would provide a superior prediction over that achieved with

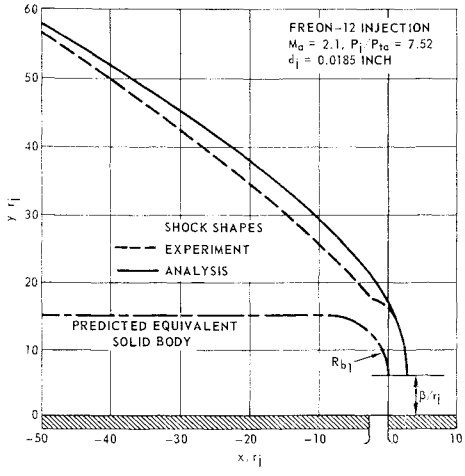

Fig. 12 Shock shape for Freon-12 injection with flash vaporization occurring.

Eq. (1a). This is indeed the case, in that the body radius predicted by the liquid penetration formula is smaller than that obtained from the BWA expression. However, the difference is not sufficient to bring the analysis and experiment into really good agreement. Thus, at this stage, we must conclude that further studies are required to produce a satisfactory analysis for cases without flash vaporization.

The Freon-12 injection experiment was at conditions such that 28% of the injectant would flash boil without heat transfer from the surrounding airstream. Here a good prediction may be anticipated, and this is demonstrated in Fig. 12. With the large amount of initial vaporization for this case, it closely approximates a gaseous injection situation. Thus, the vertical displacement of the "body" center line as predicted by the gaseous injection correlation of Fig. 2 was employed. Actually, the effect is not large for this case, and the agreement between analysis and experiment is insensitive to this refinement.

An additional point with regard to the application of the Blast Wave body radius expression to liquid injection cases should be noted. In Ref. 2, it is suggested that the effects of the heat of vaporization be accounted for by a correction factor which takes the form

$$(1 - \Delta h_v/u_a^2)^{1/2} \tag{9}$$

for an unbounded flow. This expression is developed by considering the "energy" in the blast wave to be composed of a curious combination of two distinct parts: 1) the rate of gain of axial momentum by the injectant and 2) the work done against a ficticious drag force related to the heat of vaporization. This correction factor fails severely for fluids with a high heat of vaporization; e.g., water injection into a Mach 2 airstream with 540°R total temperature where Δh_v is greater than u_a^2, producing an imaginary correction. A "correction" factor that fails in so simple a case as this must be basically deficient, and it has not been employed here. In Ref. 1, a crude extension for liquid injectants to the BWA for temperature and molecular effects is proposed. The procedure is based upon fully mixed properties and thus can only apply to the far field. Moreover, the basic extension was shown to be deficient before. Thus, this procedure is not deemed appropriate either.

Discussion

A simple, accurate procedure for calculating the interaction shock shape attending gaseous transverse injection in supersonic flow has been developed. The basic elements in the analysis are, first, the introduction of a equivalent solid body obstruction with the shape of hemisphere cylinder divided in half longitudinally lying on the body surface. The nose radius is taken as the jet penetration height (approximated by the vertical displacement of the center of the first Mach disk in the injectant) as determined from separate experiments and analysis. Second, the stagnation point of the body is raised above the body surface by a distance obtained from a nondimensional data correlation (see Fig. 2). Lastly, the shock shape past this body is predicted using the empirical formulas of Ref. 4. This whole procedure predicts the shock shape and the stand-off distance, and these predictions compare well with experiments encompassing a wide range of the pertinent variables. In particular, the important effects of injectant molecular weight and temperature are properly accounted for.

The experimental studies on the transverse injection of liquids provided shock-shape measurements for two cases: 1) water injection under conditions where flash vaporization was negligible and 2) Freon-12 injection where substantial flash vaporization could be anticipated and was observed. Thus, the first direct data on the effect of the important relation of the vapor pressure of the injectant to the pressure in the external environment surrounding the injection port were presented here. For the analysis of liquid injection cases, the successful procedure developed for gaseous injection could not be directly extended, because no comparable analysis for liquid jet penetration yet exists. Thus, we were forced to fall back upon the Blast Wave Analogy for the prediction of the body nose radius, even though it had been proven deficient with regard to variations in gaseous injectant temperature and molecular weight. These problems can be viewed as a failure to distinguish properly between injectant mass flow and volume flow. Therefore, more severe difficulties can be expected with liquid injectants, since differences between mass flow and volume flow effects may be very large for such cases. This was verified by the fact that only cases at conditions where substantial flash vaporization occurs were reasonably predicted.

On the basis of the present studies, we may conclude that a prediction procedure for the interaction shock shape with gaseous injection is in hand, while the development of an equivalent procedure for liquid injectants must await the furtherance of understanding regarding liquid jet penetration. Also, the important influences of liquid injectant vapor pressures must receive further study.

References

[1] Broadwell, J. E., "Analysis of the Fluid Mechanics of Secondary Injection for Thrust Vector Control," *AIAA Journal*, Vol. 1, No. 5, May 1963, pp. 1067–1075.

[2] Hsia, H. T.-S., Seifert, H., and Karamcheti, K., "Shock Induced by Secondary Fluid Injection," *Journal of Spacecraft and Rockets*, Vol. 2, No. 1, Jan.-Feb. 1965, pp. 67–72.

[3] Hsia, H. T-S, "Equivalence of Secondary Injection to a Blunt Body in Supersonic Flow," *AIAA Journal*, Vol. 4, No. 10, Oct. 1966, pp. 1832–1834.

[4] Billig, F. S., "Shock-Wave Shapes Around Spherical and Cylindrical-Nosed Bodies," *Journal of Spacecraft and Rockets*, Vol. 4, No. 6, June 1967, pp. 822–823.

[5] Anderson, J. D., Jr., Albacete, L. M., and Winkelmann, A. E., "Comment on Shock-wave shapes around spherical—and cylindrical-nosed bodies," *Journal of Spacecraft and Rockets*, Vol. 5, No. 10, Oct. 1968, p. 1247.

[6] Schetz, J. A., Hawkins, P. F., and Lehman, H., "Structure of Highly Underexpanded Transverse Jets in a Supersonic Stream," *AIAA Journal*, Vol. 5, No. 5, May 1967, pp. 882–884.

[7] Schetz, J. A., Weinraub, R., and Mahaffey, R., "Supersonic Transverse Injection in Supersonic Flow," *AIAA Journal*, Vol. 6, No. 5, May 1968, pp. 933–934.

[8] Orth, R. C. and Funk, J. A., "An Experimental and Comparative Study of Jet Penetration in Supersonic Flow," *Journal of Spacecraft and Rockets*, Vol. 4, No. 9, Sept. 1967, pp. 1236–1242.

[9] Chrans, L. I. and Collins, D. J., "The Effect of Stagnation

Temperature and Molecular Weight Variation of Gaseous Injection into a Supersonic Stream," AIAA Paper 69-1, New York, 1969.

[10] Dowdy, M. W. and Newton, J. F., Jr., "Investigation of Liquid and Gaseous Secondary Injection Phenomena on a Flat Plate with M = 2.01 to M = 4.54," TR 32-542, Dec. 1963, Jet Propulsion Lab.

[11] Yates, C. L. and Rice, J. L., "Liquid Jet Penetration," *Research and Development Programs Quarterly Report*, U-RQR/69-2, April-June 1969, Applied Physics Lab., Johns Hopkins Univ.

FEBRUARY 1970 J. SPACECRAFT VOL. 7, NO. 2

Applicability of Hypersonic Small-Disturbance Theory and Similitude to Internal Hypersonic Conical Flows

SANNU MÖLDER* AND NORBERT D'SOUZA†
McGill University, Montreal, Canada

The applicability of hypersonic small-disturbance theory and its attendant hypersonic similitude to internal hypersonic flows is examined by comparing the exact conical flow solutions to their small-disturbance counterparts for 1) internal conical flow axisymmetric inlets with leading edge shock (ICFA) and 2) conical flow, Busemann-type axisymmetric inlets. The associated small-disturbance hypersonic similarity law is demonstrated for these internal flows. The results shown are for ideal gas flows in inlets with sharp leading edge. The surface pressures for Busemann inlet are compared with the available experimental data. A convenient method, based on hypersonic similitude, is presented for calculating Busemann-type inlet shapes.

Nomenclature

C_p = pressure coefficient = $2(p - p_\infty)/\rho_\infty U_\infty^2$
D = inlet diameter
f = part of the stream function [See Eq. (6a)]
j = constant which is zero for two-dimensional flow, unity for axially symmetric flow
K = hypersonic similarity parameter
l = length
M = Mach number
p = pressure
r = radius in cylindrical or spherical coordinates
R = characteristic inlet radius
t = time
T = temperature
u,v = velocity components in cylindrical or spherical coordinates
U = streamwise reference velocity
x,r = Cartesian coordinates with x in streamwise direction
y = transverse distance measured from the streamwise axis through the leading edge
α = conical variable = $\tan^{-1}\sigma$
γ = ratio of specific heats
δ = body deflection angle
θ = angle measured from x axis
ξ = nondimensional longitudinal distance
ρ = density
σ = conical variable = $\bar{r}/\bar{x}$
τ = body or shock slope
ω = entropy function
ψ = stream function
ζ = see Eq. (10)
Γ = see Eq. (17)

Subscripts

0 = refers to shock or leading edge
2,3 = upstream and downstream conditions for shock, respectively
t, ∞ = total and freestream conditions, respectively

Superscripts

$(\bar{\ })$ = dimensionless form
$(\ )'$ = derivative with respect to conical variable σ
$(\dot{\ })$ = derivative with respect to α
$(\ )^*$ = value at the singular line

Received May 8, 1969; revision received August 6, 1969. This work has been financially supported by National Research Council Grant 4190.

* Associate Professor, Department of Mechanical Engineering. Member AIAA.

† Research Assistant and Commonwealth Scholar, Department of Mechanical Engineering.

Introduction

THE hypersonic small-disturbance theory (HSDT) is based on the assumptions that the slope of the local surface of the body in the streamwise direction is everywhere small compared with unity; the velocity perturbations are small compared with the freestream velocity, and the pressure perturbations are small compared with the freestream dynamic pressure. However, the velocity perturbations are not small compared with the freestream sonic speed, and pressure perturbations are not small compared with the freestream static pressure.

The usefulness of HSDT and the resulting hypersonic similitude arises from the fact that the body or shock slope parameter, τ, can be combined with the freestream Mach number, M_∞, and the independent variables, thereby simplifying the basic conservation equations. This can be done for τ sufficiently small and $M_\infty\tau$ of the order unity. Hypersonic similitude arises directly from the HSDT. It relates flows past similarly shaped bodies at different M_∞'s when $K = M_\infty\tau$ is kept constant, thus reducing the number of independent parameters by one.

Solution of the HSDT equations and the existence of the similarity law have been amply demonstrated for flow over wedges, cones and ogives.[1,2] Since the assumptions involved